Dose-Response:
An International Journal
April-June 2020:1-9

DOI: 10.1177/1559325820936906
journals.sagepub.com/home/dos
SAGE

MiR-1587 Regulates DNA Damage Repair and the Radiosensitivity of CRC Cells via Targeting LIG4

Ruixue Liu[1,2], Liping Shen[2], Chuxian Lin[2], Junyan He[2], Qi Wang[2], Zhenhua Qi[2], Qingtong Zhang[3], Meijuan Zhou[1], and Zhidong Wang[2]

Abstract

DNA is subject to a range of endogenous and exogenous insults that can impair DNA replication and lead to DNA double-strand breaks (DSBs). The repair capacity of cancer cells mediates their radiosensitivity, but the roles of miR-1587 during radiation resistance are poorly characterized. In this study, we explored whether miR-1587 regulates the growth and radiosensitivity of colorectal cancer (CRC) cells through its ability to regulate DNA Ligase4 (LIG4). We found that CRC cells in which miR-1587 was overexpressed inhibited cell growth and promoted apoptosis through increasing DSBs and promoting cell cycle arrest. We found that overexpression of miR-1587 significantly inhibited LIG4 messenger RNA and protein expression and further revealed the ability of miR-1587 to directly bind to the LIG4-3′-untranslated region through dual-luciferase reporter assays. More notably, miR-1587 mimics increased the radiosensitivity of CRC cells. Taken together, we show that miR-1587 overexpression enhances the formation of DSBs, arrests CRC cell growth, and enhances the radiosensivity of CRC cells through the direct repression of LIG4 expression. These results reveal novel roles for miR-1587 during DNA damage repair and the radiosensivity of CRC cells. This highlights miR-1587 as a novel therapeutic target for CRC.

Keywords

DNA double-strand breaks, radiosensitivity, miR-1587, LIG4

Introduction

DNA damage can result from intrinsic (reactive oxygen species) and extrinsic stresses (ionizing radiation and chemotherapy drugs). DNA double-strand breaks (DSBs) are the most severe form of DNA damage as they promote genomic instability.[1,2] Genome stability requires the integrity of the DNA repair machinery. DNA double-strand breaks are repaired by homologous recombination (HR) and non-homologous end-joining (NHEJ).[3] Homologous recombination repair occurs during the S and G2 phases of the cell cycle and repairs single-terminal DSBs during DNA replication. Non-homologous end-joining repair occurs throughout the cell cycle, particularly during the G1 phase. Essential proteins in the NHEJ repair pathway include DNA-PK, KU70, KU80, XRCC4, XLF, and DNA Ligase4 (LIG4).[4,5] DNA Ligase4 is key to the formation of terminal links.

Subsets of patients with colorectal cancer (CRC) show resistance to radiation therapy leading to poor treatment outcomes.[6,7] The causes of radiotherapy resistance include the protective nature of the tumor microenvironment, impaired

[1] Department of Radiation Medicine, Guangdong Provincial Key Laboratory of Tropical Disease Research, School of Public Health, Southern Medical University, Guangzhou, People's Republic of China
[2] Department of Radiobiology, Beijing Key Laboratory for Radiobiology, Beijing Institute of Radiation Medicine, Beijing, People's Republic of China
[3] Department of Colorectal Surgery, Cancer Hospital of China Medical University, Liaoning Cancer Hospital & Institute, People's Republic of China

Received 12 January 2020; received revised 19 February 2020; accepted 25 February 2020

Corresponding Authors:
Zhidong Wang, Department of Radiobiology, Beijing Key Laboratory for Radiobiology, Beijing Institute of Radiation Medicine, No. 27, Taiping Road, Haidian District, Beijing, 100850, People's Republic of China.
Email: wangzhidong_1977@aliyun.com

Meijuan Zhou, Department of Radiation Medicine, Guangdong Provincial Key Laboratory of Tropical Disease Research, School of Public Health, Southern Medical University, No.1023, Shatai South Road, Baiyun District, Guangzhou 510515, People's Republic of China.
Email: lkzmj@smu.edu.cn

Qingtong Zhang, Department of Colorectal Surgery, Cancer Hospital of China Medical University, Liaoning Cancer Hospital & Institute, No.44 Xiaoheyan Road, Dadong District, Shenyang 110042, People's Republic of China.
Email: 26909601111@qq.com

DNA damage responses, and damaged DNA repair ability. Exploring the molecular mechanisms of radiation-induced DNA damage repair is of great clinical significance for CRC treatment.

MicroRNAs (miRNAs) are small noncoding RNAs (20-24 nucleotides in length) that control the translation and stability of cellular messenger RNAs (mRNAs) through binding to 3′-untranslated region (3′UTR) regions.[8-11] miRNAs are important posttranscriptional regulators of gene expression and regulate a variety of biological processes, including cell proliferation, differentiation, and cancer progression.[12,13] Increasing evidence supports a role for miRNAs in the regulation of DNA damage repair.[14,15] However, the impact of miR-1587 on both DNA repair and radiation sensitivity in CRC cells remains uncharacterized.

In our experiments on the function of lnc-RI, we found that miR-1587 could simultaneously target lnc-RI and LIG4, so we speculated whether miR-1587 could regulate DNA damage repair and radiological sensitivity by regulating LIG4 expression. In this study, we confirmed that miR-1587 overexpression inhibits the proliferation of CRC cells and promotes apoptosis. And overexpression of miR-1587 increased the number of endogenous DSBs and induced G1 phase arrest. As a key molecule in the NHEJ pathway, LIG4 expression was strongly repressed in CRC cells expressing miR-1587 mimics and we demonstrated that miR-1587 directly targets the LIG4 mRNA 3′-UTR. In addition, the transfection of miR-1587 mimics significantly increased the radiosensitivity of HT29 cells. These results reveal new mechanistic insight into the DNA damage repair processes of CRC cells and identify miR-1587 as a potent ionizing radiation (IR) sensitizing agent.

Materials and Methods

Cell Culture

HCT116 and HT29 cells were purchased from the Cell Bank of Chinese Academy of Sciences. HCT116 cells were grown in RPMI-1640 (HyClone). HT29 cells were grown in high glucose DMEM (HyClone) supplemented with 10% (vol/vol) fetal bovine serum (ExCell Bio, Cat. No. FSP500), 100 units/mL penicillin, and 100 μg/mL streptomycin (HyClone). Cells were grown in a humidified incubator at 37 °C with 5% CO2.

Primers and miRNA Mimics

U6, forward 5′-CTCGCTTCGGCAGCACA-3′ and reverse 5′-AACGCTTCACGAATTTGCGT-3′ primers were synthesized by TsingKe Biological Technology, and miR-1587 primers were designed and synthesized by RiboBio. MiR-1587 mimics (sense: 5′-UUGGGCUGGGCUGGGUUGGG-3′, antisense: 5′-CAA CCCAGCCCAGCCCAAUU-3′); miR-NC (sense: 5′-UUCU CCGAACGUGUCACGUTT-3′, antisense: 5′-ACGUGACA CGUUCGGAGAATT-3′) were synthesized by Shanghai GenePharma Company.

Cell Transfection

Cells were seeded into 6-well plates and transfected with miRNA mimics or negative controls using Lipofectamine 2000 (Invitrogen) according to the manufacturer's protocols. Plasmids were transfected using jetPRIME Transfection Reagent (Polyplus transfection) according to the manufacturer's protocols.

Clinical Sample Acquisition

Clinical samples of CRC tissue were obtained from the Department of Colorectal Surgery, Cancer Hospital of China Medical University. Of the 20 cases assessed, 8 were males and 12 were females, with an age range of 29 to 81 years. All patients were diagnosed with CRC and tumor tissues and adjacent tissues were obtained during surgery. All experiments were performed with the informed consent of patients and reviewed by our ethics committee.

Cell Proliferation Assays

Cell proliferation was assessed using cell counting kit-8 (CCK-8; Dojindo) as per the manufacturer's recommendations. HCT116 and HT29 cells were seeded into 96-well plates (1000 cells/well) and transfected with miR-1587 mimics or miR-NC and cultured at 37 °C in 5% CO_2 for 0, 1, 2, and 3 days post-transfection. Cell viability was assessed at the indicated time points ($n = 5$ per sample). Optical densities were measured on a microplate reader (Sunrise, Tecan) at 450 nm.

Clonogenic Cell Survival Assays

Clonogenic cell survival assays were performed to assess the effects of miR-1587 on HCT116 and HT29 cell growth. Cells were transfected with miR-1587 mimics or miR-NC for 48 hours and trypsinized and reseeded into 6-well plates at a density of 500 cells/well. Cells were incubated for 2 weeks under normal cell culture conditions, and the media was replaced every 5 days. Cells were fixed in methanol and stained with Giemsa. Microscopic colonies of $\geq$50 cells were manually counted and images were acquired on an image scanner.

Apoptosis Assays

HCT116 and HT29 cells were seeded into 24-well plates at a density of 5×10^4 cells/well, transfected with miR-1587 mimics or miR-NC, and collected 48 hours post-transfection. Annexin V-fluorescein isothiocyanate (FITC) apoptosis detection kits (Dojindo) were used to detect apoptosis in each group. Apoptotic rates were analyzed by flow cytometry (ACEA Bio). A minimum of 10 000 events per sample were recorded.

Cell Cycle Analysis

Cells were seeded into 24-well plates (5×10^4 cells/well) and transfected with miR-1587 mimics or miR-NC. At 48 hours

post-transfection, cells were collected and fixed in 70% (vol/vol) ethanol overnight at −20 °C. Samples were washed twice with phosphate-buffered saline (PBS) and incubated with 200-μL PBS containing 100 μg/mL RNaseA and 50 μg/mL propidium iodide (PI) for 30 minutes at 37 °C. Cells cycle distributions were analyzed by flow cytometry (ACEA Bio). A minimum of 10 000 events per sample were recorded.

RNA Extraction and Real-Time Quantitative Polymerase Chain Reaction

Total RNA was extracted from the cells using Trizol reagent (Sigma) according to the manufacturer's protocols. Both RNA concentration and purity were measured on an ultraviolet spectrophotometer (GE Healthcare GeneQuant 100). Total RNA (1 μg) was reverse transcribed into complementary DNA using the PrimeScriptRT reagent kit with gDNA Eraser[Please note that "Gdna" has been changed to "gDNA." Please check if this is correct.] (TaKaRa). Real-time quantitative polymerase chain reactions (RT-qPCRs) were performed using iTaq Universal SYBR Green Supermix (Bio-Rad) for mature miRNAs and mRNAs on a Bio-Rad Real-Time PCR System. U6 served as the internal control. Samples were assessed in triplicate from 3 independent experiments. Relative fold changes in expression were calculated using the $2^{-\Delta\Delta Ct}$ method.

Western Blot Analysis

Cells were harvested in 0.25% trypsin (HyClone) and washed twice in ice-cold PBS. Total proteins were extracted in lysis buffer supplemented with protease and phosphatase inhibitors (Roche Applied Science). Protein concentrations were determined via BCA Assays (Beyotime Biotechnology). Samples were denatured in sodium dodecyl sulphate (SDS) sample buffer. Total protein extracts were separated by SDS-polyacrylamide gel electrophoresis and transferred to nitrocellulose membranes. Membranes were blocked in 5% nonfat dry milk in Tris-buffered saline-containing Tween-20 (TBST) and probed overnight at 4 °C with the indicated primary antibodies. The primary antibodies used in the study included: anti-β-Actin (60008-1-lg; Proteintech), anti-γ-H2AX ser139 (05-636; Millipore), and anti-LIG4 (12695-1-AP; Proteintech). Membranes were washed in TBST and labeled with the indicated horseradish peroxidase–conjugated secondary antibodies (KPL). Membranes were washed in TBST and protein bands were visualized using the Image Quant LAS500 system (GE Healthcare).

Immunofluorescence Assays

Cells seeded onto coverslips in 6-well plates (2.8×10^5 cells per well) were treated with miR-1587 mimics or miR-NC. After 48 hours, cells were fixed in 4% paraformaldehyde, permeabilized in 0.3% Triton X-100 in PBS, and blocked in 3% bovine serum albumin in PBS. Subsequently, cells were immunostained with anti-γ-H2AX (1:400; Millipore) primary antibodies overnight at 4 °C in a humidified environment. Cells were washed and labeled with FITC-conjugated anti-IgG antibodies (1:400; KPL) at room temperature for 2 hours. Nuclei were visualized with 4, 6-diamidino-2-phenylindole–staining (2 μg/mL) for 10 minutes in the dark. Images were acquired using a Nikon Ti-A1 capture system (magnification, 60×). The number of γ-H2AX foci per nucleus was counted.

Dual Luciferase Reporter Assay

Inserted sequences (70-276 bp) of the LIG4 mRNA 3′UTR were cloned into pmirGLO, which simultaneously expresses Firefly luciferase and Renilla luciferase as internal control. Wild-type LIG4-3′UTR sequences were designated pmirGLO-LIG4-3′UTR-wt and mutated LIG4-3′UTR sequences lacking the miR-1587 binding site were designated pmirGLO-LIG4-3′UTR-mu constructs. Plasmids were synthesized by TsingKe Biological Technology. Cells were seeded into 24-well plates (5.0×10^4 cells per well) 24 hours prior to transfection. Constructs were co-transfected into cells with either miR-1587 mimics or control NC. After incubation for 48 hours, cells were lysed and luciferase assays were performed using a Dual-Luciferase Reporter Assay System (Promega). Firefly luciferase activity was normalized to Renilla luciferase values. Each group were assayed in triplicate.

Cell Irradiation

Cultured cells were irradiated with the specified radiation doses using ^{60}Co γ-rays at a dose rate of 62.3 cGy/min at room temperature.

Statistical Analysis

Data are shown as the mean ± SD (all experiments were performed on a minimum of 3 independent occasions). Groups were compared using a 2-tailed Student *t* test (*$P < .05$, **$P < .01$, or ***$P < .001$ were considered statistically significant, NS means no significance). Error bars indicate the SEM.

Results

MiR-1587 Inhibits CRC Cells Growth and Promotes Apoptosis

We detected the expression of miR-1587 in CRC cell lines and clinical samples and found that the expression of miR-1587 was significantly lower in CRC tissue and tumor cells compared to adjacent healthy tissue and normal colon cells (Figure S1). We therefore speculated that miR-1587 might inhibit tumor cell growth. As shown in Figure 1A, cells expressing miR-1587 mimics showed increased levels of miR-1587 expression. We investigated the effects of miR-1587 on CRC cell proliferation using CCK-8 assays from 0 to 3 days post-transfection (Figure 1B). The results showed that cell proliferation significantly decreased and changes in cell morphology

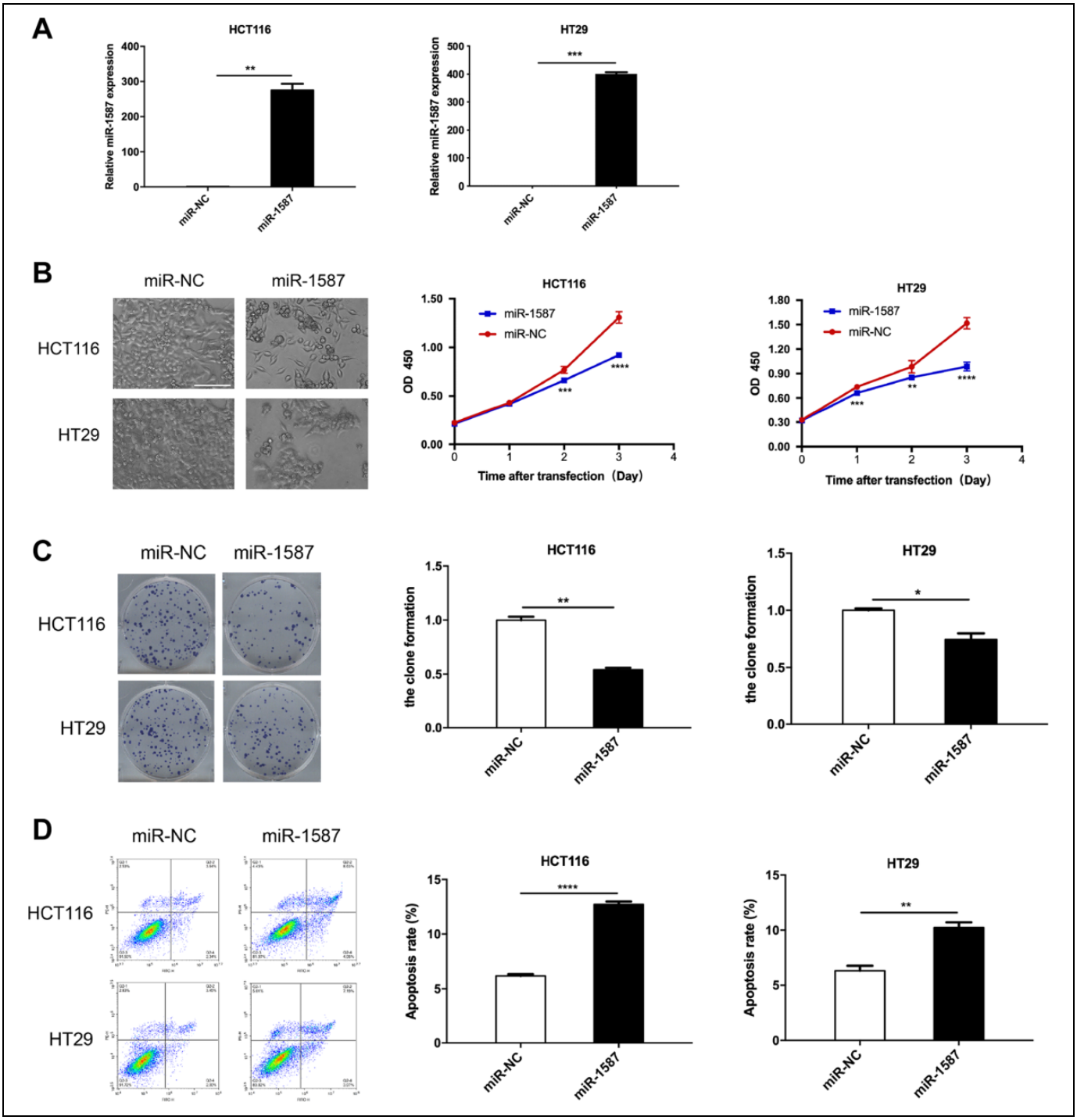

Figure 1. Overexpression of miR-1587 inhibits proliferation and promotes apoptosis of CRC cells. A, Identification of miR-1587 overexpression. Cells were transfected with miR-1587 or miR-NC mimics. After 48 hours, miR-1587 expression was detected by RT-qPCR. U6 was used as an internal control. *t* test, mean ± SD, n = 3. B, MiR-1587 inhibits the proliferation of CRC cells. Cells were seeded into 96-well plates and transfected with miR-1587 or miR-NC mimics. Cell proliferation was measured via CCK-8 assays at the indicated time points. Cells morphologies were assessed via microscopy. Scale bar: 300 μm. *t* test, mean ± SD, n = 5. C, MiR-1587 overexpression regulates CRC clone formation. CRC cells transfected with miR-1587 or miR-NC mimics for 48 hours and reseeded at low density into 6-well plates, and colony-formation assays were performed after 14 days. *t* test, mean ± SD, n = 3. D, MiR-1587 overexpression promotes CRC cells apoptosis. Cells were transfected with miR-1587 and miR-NC mimics for 48 hours and apoptosis was assessed by flow cytometry. **P* < .05, ***P* < .01, ****P* < .001. CCK-8 indicates cell counting kit-8; CRC, colorectal cancer; RT-qPCR, real-time quantitative polymerase chain reaction.

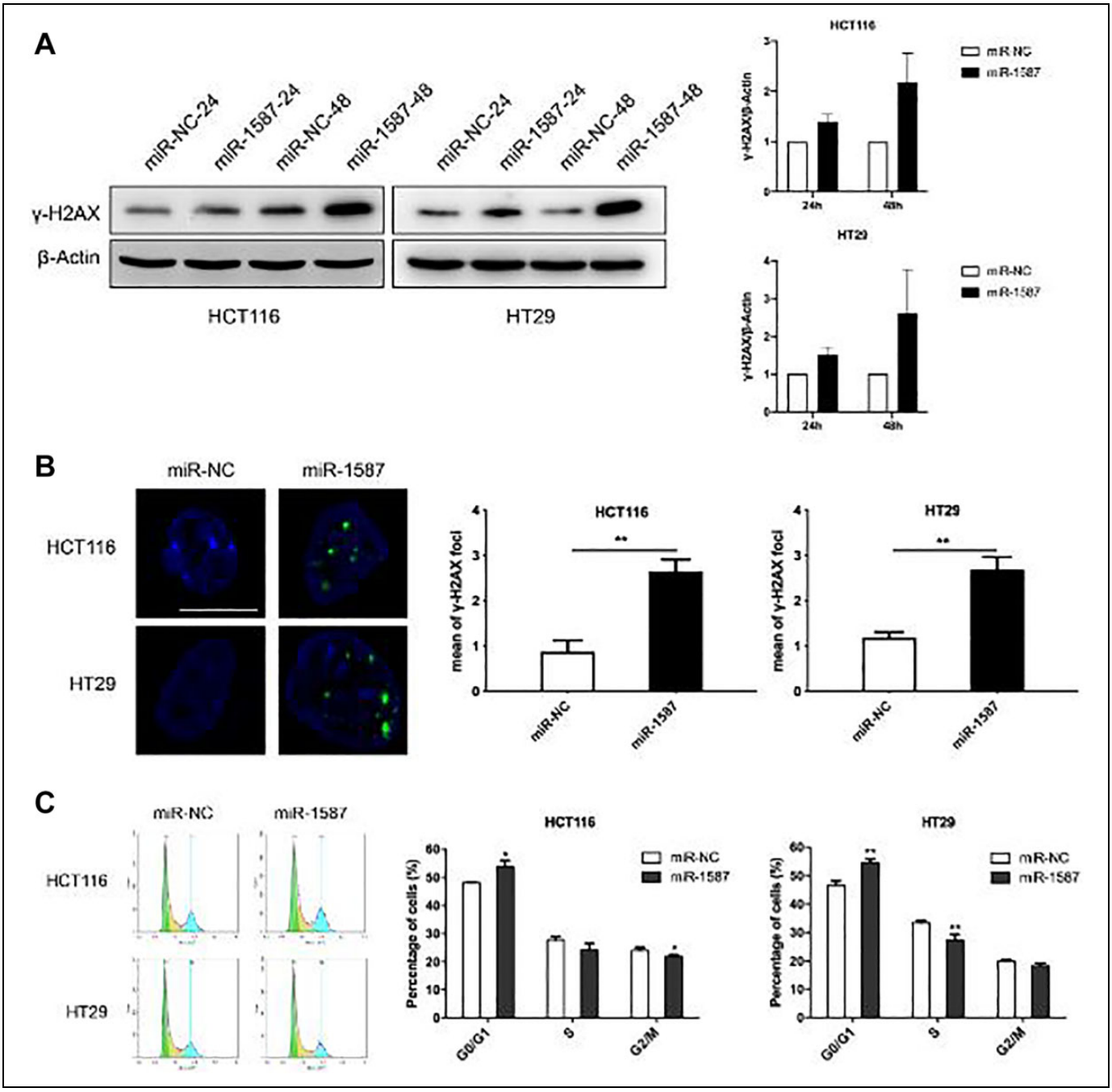

Figure 2. Overexpression of miR-1587 induces CRC cells DSBs and induces G1 phase arrest. A, MiR-1587 enhances γ-H2AX expression. CRC cells were transfected with miR-1587 or miR-NC mimics for 48 hours and the expression of γ-H2AX was detected by Western blot analysis (left). The protein was quantified by gray-scale statistics (right). B, Overexpression of miR-1587 triggers the formation of γ-H2AX foci. CRC cells were seeded onto coverslips in 6-well plates and transfected with miR-1587 or miR-NC mimics for 48 hours. γ-H2AX foci were detected by indirect immunofluorescence staining from a minimum of 200 randomly selected cells in each group. Scale bar: 20 μm. *t* test, mean ± SD, n = 200. C, MiR-1587 overexpression induces G1 phase arrest. CRC cells were transfected with miR-1587 or miR-NC mimics for 48 hours and the cell cycle analysis was performed via flow cytometry. A total of 10 000 cells in each sample were scored. *t* test, mean ± SD, n = 3. **P* < .05, ***P* < .01, and ****P* < .001. CRC indicates colorectal cancer; DSB, DNA double-strand break.

and density were apparent between miR-1587 mimics and control NC groups. The effects of miR-1587 on cell growth were further verified by clonogenic assays. As predicted, miR-1587 mimics significantly inhibited CRC cell colony formation (Figure 1C) compared to control miR-NC treated cells. We further explored the role of miR-1587 during CRC cell apoptosis. At 48 hours postinfection, cell apoptosis was detected by flow cytometry of Annexin V-conjugated FITC/PI-stained cells. The levels of apoptosis in miR-1587 mimic groups were significantly higher than those of the miR-NC group (Figure 1D).

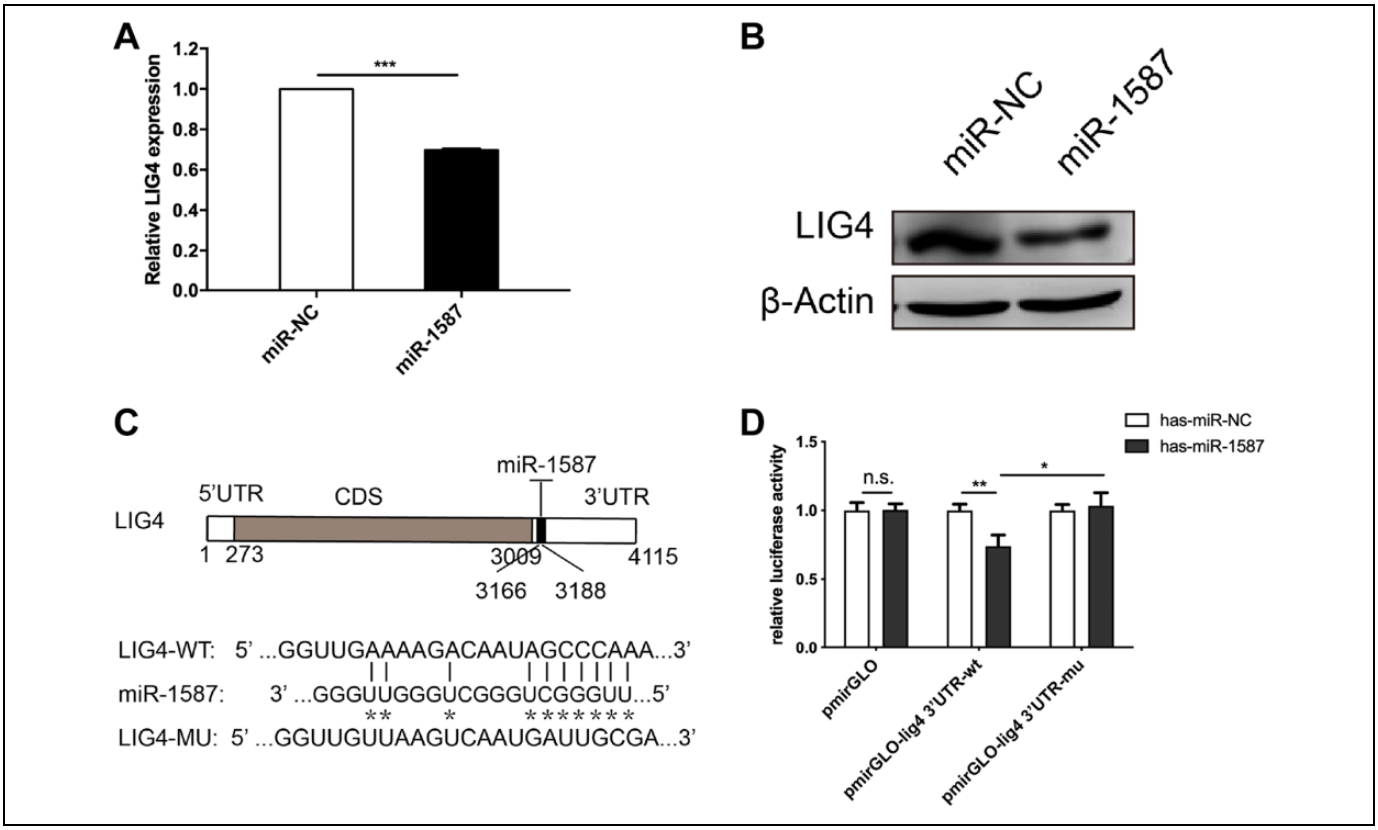

Figure 3. MiR-1587 regulates LIG4 expression through direct targeting of the LIG4-3′UTR. A and B, MiR-1587 mimics suppressed LIG4 mRNA and protein expression. HCT116 cells were transfected with miR-1587 or miR-NC mimics for 48 hours and the relative expression of LIG4 was detected by RT-qPCR. *t* test, mean ± SD, n = 3. Expression of LIG4 assessed via Western blot analysis. C, Predicted target sites of miR-1587 in LIG4 mRNA 3′UTR. Luciferase reporter vectors were constructed by cloning wild-type and mutated LIG4 mRNA 3′UTR sequences targeted by miR-1587 into pmirGLO plasmids. D, MiR-1587 directly targets the LIG4 mRNA 3′UTR. HCT116 cells were co-transfected with reporter vectors and miR-1587 or miR-NC mimics. Luciferase activity was measured 48 hours post transfection. *t* test, mean ± SD, n = 3. **P* < .05, ***P* < .01, ****P* < .001. CRC indicates colorectal cancer; mRNA, messenger RNA; RT-qPCR, real-time quantitative polymerase chain reaction; 3′UTR, 3′ untranslated region.

These data suggest that miR-1587 plays a key role in the survival of CRC cells.

MiR-1587 Induces CRC Cell DSBs and Cell Cycle Arrest

To monitor DNA damage in CRC cells, the number of γ-H2AX foci as a marker of DSBs was assessed. In CRC cells transfected with miR-1587 mimics, increased γ-H2AX expression was observed (Figure 2A). We performed a quantitative determination of γ-H2AX foci in CRC cells following transfection with miR-1587 mimics or miR-NC for 48 hours. As shown in Figure 2B, a significantly increased yield of γ-H2AX foci was observed in CRC cells expressing miR-1587 mimics compared to those expressing miR-NC. The enhanced expression of γ-H2AX and increased foci formation further inferred an induction of DSBs. DNA damage triggers cell cycle arrest as a protective response to allow cells time to repair prior to cell division.[16,17] We found that upon transfection with miR-1587 mimics, HCT116 and HT29 cells showed enhanced G1 arrest (Figure 2C). Taken together, we conclude that miR-1587 overexpression induces DSBs in CRC cells resulting in a delay in G1 progression.

MiR-1587 Regulates LIG4 Expression by Directly Targeting the LIG4-3′UTR

RT-qPCR analysis showed that LIG4 expression was downregulated in CRC cells, while miR-1587 was upregulated compared to the miR-NC group (Figure 3A). These findings were confirmed by Western blot analysis (Figure 3B). MicroRNAs bind to the 3′UTR region of target mRNAs to facilitate their degradation and/or inhibit protein translation. To confirm a direct interaction of miR-1587 with the LIG4 mRNA 3′UTR, pmirGLO-LIG4-3′UTR-wt and pmirGLO-LIG4-3′UTR-mu reporter vectors were constructed. The predicted miR-1587 targeting site and sequence of the LIG4 mRNA 3′UTR are shown in Figure 3C. The 3′UTR region of LIG4 mRNA containing the miR-1587 targeting sequence and its mutant were independently cloned downstream of luciferase in the pmirGLO plasmid. Cells were co-transfected with the reporter vectors and miR-1587 mimics or miR-NC. Dual-luciferase assays

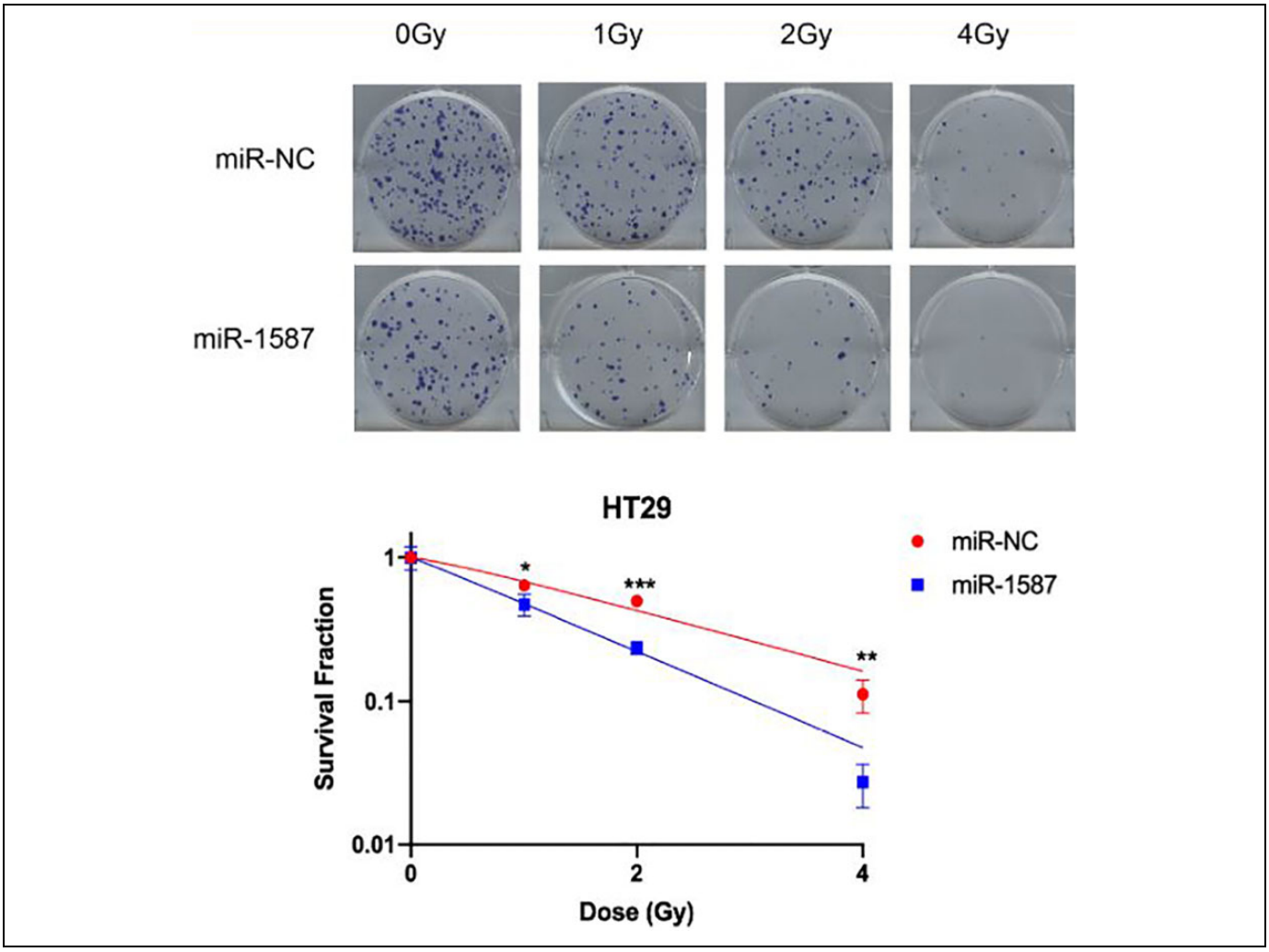

Figure 4. Overexpression of miR-1587 enhances the radiosensitivity of HT29 cells. MiR-1587 overexpression enhances the radiosensitivity of HT29 cells. After transfection with miR-1587 or miR-NC mimics for 48 hours, HT29 cells were collected and reseeded into 6-well plates, and colony-formation assays were performed following irradiation (0, 1, 2, and 4 Gy) for 2 weeks. *t* test, mean ± SD, n = 3. **P* < .05, ***P* < .01, ****P* < .001.

showed that miR-1587 inhibited the activity of pmirGLO-LIG4-3′UTR-wt but had little influence on pmirGLO-LIG4-3′UTR-mu reporters (Figure 3D). Thus, miR-1587 directly interacts with the LIG4 mRNA 3′UTR to regulate LIG4 expression.

MiR-1587 Enhances the Radiosensitivity of CRC Cells

The repair of DNA damage is closely related to the radiosensitivity of cancer cells.[18,19] MiR-1587 overexpression induces DSBs in both HCT116 and HT29 cells (Figure 2A-B) and so it was predicted that the expression of miR-1587 correlates with the radiosensitivity of CRC cells. Following transfection with miR-1587 mimics, clonogenic ability at different radiation doses of 0, 1, 2, and 4 Gy was assessed in HT29 cells and the parameters of a multitarget/single-hit models based on the clonogenic survival assays were calculated. The results (Figure 4 and Table 1) indicated that miR-1587 increased the radiosensitivity of HT29 cells compared to miR-NC groups, confirming its role in the radiosensitivity of CRC cells. These results provided evidence that miR-1587 mimics are an effective small molecule target to enhance the therapeutic regimens of patients with CRC.

Table 1. The Main Parameters of a Multi-Target Model Based on Colony-Formation Assays.

	N	D0	Dq	SER
HT29-miR-NC	1.219	1.996	0.395	
HT29-miR-1587	1.044	1.296	0.056	7.081

Abbreviations: N, extrapolation number; D0, mean lethal dose; Dq, quasi-threshold dose; SER, sensitivity enhancement ratio.

Discussion

An increasing body of the literature highlights the roles of miRNAs in a variety of biological processes. Accordingly,

their dysregulation is associated with human disease.[20,21] MiR-21 mediates drug and radiation resistance through the regulation of DNA damage repair (including HR and NHEJ repair).[22] Exosome miR-1246 inhibits the efficiency of NHEJ repair and leads to DNA damage through targeting LIG4.[23] However, studies in this area are still limited. Here, we report that miR-1587, a novel molecule in the DNA damage repair and radiosensitivity of cancer cells, directly binds to the LIG4-3′UTR and inhibits LIG4 expression, leading to endogenous DNA damage that positively correlates with the radiosensitivity of CRC cells.

DNA double-strand breaks lead to severe DNA damage due to IR and harmful metabolites, with NHEJ the main repair pathway to repair the double-stranded structures caused by DSBs.[24] DNA Ligase4 is key to the NHEJ repair pathway and is necessary for the formation of terminal links. It has been reported that LIG4 dysfunction leads to immune deficiency, developmental delay, neurodegeneration, and cancer formation.[25-27] In this study, we confirmed that the overexpression of miR-1587 significantly inhibits the growth of CRC cells and promotes apoptosis. Increasing the levels of endogenous DSBs leads to G1 arrest. Interestingly, following the overexpression of miR-1587, the expression of LIG4, a key molecule of the NHEJ repair pathway, was inhibited. Dual luciferase reporter gene assays confirmed that miR-1587 directly targets the LIG4-3′UTR to regulate LIG4 expression. Moreover, the overexpression of miR-1587 increased the radiosensitivity of HT29 cells. To our knowledge, this is the first report highlighting the role of miR-1587 in DNA damage repair. An increasing number of studies have confirmed that the repair of DSBs is a key factor in radiosensitivity during radiotherapy[28-30] and that the inhibition of tumor repair directs anticancer therapy.[31] MiR-1587 may therefore represent an effective target for CRC therapy.

In summary, we demonstrate that miR-1587 plays an important role in DNA damage repair in CRC cells through targeting LIG4. This highlights miR-1587 mimics as a potential strategy for CRC therapeutics through their ability to inhibit DNA damage repair in tumor cells, promoting cell death in response to radiotherapy. This highlights the potential of miRNAs to enhance or overcome radiation and/or drug resistance in cancer cells.[32,33]

Conclusion

In conclusion, our study indicates that miR-1587 overexpression increases DSBs and radiosensitivity via downregulating LIG4 expression. The inhibitory effects of miR-1587 on LIG4 are attributed to the direct binding to LIG4-3′UTR. It suggests that miR-1587 as a potential target in radiotherapy of CRC.

Declaration of Conflicting Interests

The author(s) declared no potential conflicts of interest with respect to the research, authorship, and/or publication of this article.

Funding

The author(s) disclosed receipt of the following financial support for the research, authorship, and/or publication of this article: This work was supported by grants from National Natural Science Foundation of China [31770913 to Z.W.].

Supplemental Material

Supplemental material for this study is available online.

References

1. Cameron AM, Castoldi A, Sanin DE, et al. Inflammatory macrophage dependence on NAD+ salvage is a consequence of reactive oxygen species–mediated DNA damage. *Nat Immunol*. 2019; 20(4):420-432.
2. Nikitaki Z, Mavragani IV, Laskaratou DA, et al. Systemic mechanisms and effects of ionizing radiation: a new 'old' paradigm of how the bystanders and distant can become the players. *Semin Cancer Biol*. 2016;37-38:77-95.
3. Goldstein M, Kastan MB. The DNA damage response: implications for tumor responses to radiation and chemotherapy. *Annu Rev Med*. 2015;66(1):129-143.
4. Jiang N, Shen Y, Fei X, et al. Valosin-containing protein regulates the proteasome-mediated degradation of DNA-PKcs in glioma cells. *Cell Death Dis*. 2013;4(5):e647.
5. Conlin MP, Reid DA, Small GW, et al. DNA ligase IV guides end-processing choice during nonhomologous end joining. *Cell Rep*. 2017;20(12):2810-2819.
6. Baker B, Salameh H, Al-Salman M, Daoud F. How does preoperative radiotherapy affect the rate of sphincter-sparing surgery in rectal cancer? *Surg Oncol*. 2012;21(3):e103-e109.
7. Kawai K, Ishihara S, Nozawa H, et al. Prediction of pathological complete response using endoscopic findings and outcomes of patients who underwent watchful waiting after chemoradiotherapy for rectal cancer. *Dis Colon Rectum*. 2017;60(4):368-375.
8. Wan G, Mathur R, Hu X, Zhang X, Lu X. miRNA response to DNA damage. *Trends Biochem Sci*. 2011;36(9):478-484.
9. van Kouwenhove M, Kedde M, Agami R. MicroRNA regulation by RNA-binding proteins and its implications for cancer. *Nat Rev Cancer*. 2011;11(9):644-656.
10. Friedman RC, Farh KKH, Burge CB, Bartel DP. Most mammalian mRNAs are conserved targets of microRNAs. *Genome Res*. 2008;19(1):92-105.
11. Hausser J, Zavolan M. Identification and consequences of miRNA–target interactions—beyond repression of gene expression. *Nat Rev Genet*. 2014;15(9):599-612.
12. Zhang Z, Zhang C, Li F, Zhang B, Zhang Y. Regulation of memory CD8+ T cell differentiation by microRNAs. *Cell Physiol Biochem*. 2018;47(6):2187-2198.
13. Polytarchou C, Hommes DW, Palumbo T, et al. MicroRNA214 is associated with progression of ulcerative colitis, and inhibition reduces development of colitis and colitis-associated cancer in mice. *Gastroenterology*. 2015;149(4):981-992.
14. He M, Lin Y, Tang Y, et al. miR-638 suppresses DNA damage repair by targeting SMC1A expression in terminally differentiated cells. *Aging (Albany NY)*. 2016;8(7):1442-1456.

15. Lee J, Park S, Jeong S, et al. MicroRNA-22 suppresses DNA repair and promotes genomic instability through targeting of MDC1. *Cancer Res*. 2015;75(7):1298-1310.
16. Barshishat S, Elgrably-Weiss M, Edelstein J, et al. OxyS small RNA induces cell cycle arrest to allow DNA damage repair. *EMBO J*. 2018;37(3):413-426.
17. Chao HX, Poovey CE, Privette AA, et al. Orchestration of DNA damage checkpoint dynamics across the human cell cycle. *Cell Syst*. 2017;5(5):445-459.
18. Pajic M, Froio D, Daly S, et al. miR-139-5p modulates radiotherapy resistance in breast cancer by repressing multiple gene networks of DNA repair and ROS defense. *Cancer Res*. 2018;78(2):501-515.
19. Thangavel C, Boopathi E, Ciment S, et al. The retinoblastoma tumor suppressor modulates DNA repair and radioresponsiveness. *Clin Cancer Res*. 2014;20(21):5468-5482.
20. Ebert MS, Sharp PA. Roles for microRNAs in conferring robustness to biological processes. *Cell*. 2012;149(3):515-524.
21. Rupaimoole R, Calin GA, Lopez-Berestein G, Sood AK. miRNA deregulation in cancer cells and the tumor microenvironment. *Cancer Discov*. 2016;6(3):235-246.
22. Hu B, Wang X, Hu S, et al. miR-21-mediated radioresistance occurs via promoting repair of DNA double strand breaks. *J Biol Chem*. 2017;292(8):3531-3540.
23. Mo LJ, Song M, Huang QH, et al. Exosome-packaged miR-1246 contributes to bystander DNA damage by targeting LIG4. *Br J Cancer*. 2018;119(4):492-502.
24. Pannunzio NR, Watanabe G, Lieber MR. Nonhomologous DNA end-joining for repair of DNA double-strand breaks. *J Biol Chem*. 2018;293(27):10512-10523.
25. O Driscoll M, Gennery AR, Seidel J, Concannon P, Jeggo PA. An overview of three new disorders associated with genetic instability: LIG4 syndrome, RS-SCID and ATR-seckel syndrome. *DNA Repair*. 2004;3(8-9):1227-1235.
26. Jackson SP, Bartek J. The DNA-damage response in human biology and disease. *Nature*. 2009;461(7267):1071-1078.
27. Lieber MR, Ma Y, Pannicke U, Schwarz K. Mechanism and regulation of human non-homologous DNA end-joining. *Nat Rev Mol Cell Bio*. 2003;4(9):712-720.
28. Rube CE, Grudzenski S, Kuhne M, et al. DNA double-strand break repair of blood lymphocytes and normal tissues analysed in a preclinical mouse model: implications for radiosensitivity testing. *Clin Cancer Res*. 2008;14(20):6546-6555.
29. Tarish FL, Schultz N, Tanoglidi A, et al. Castration radiosensitizes prostate cancer tissue by impairing DNA double-strand break repair. *Sci Transl Med*. 2015;7(312):311r-312r.
30. Hatano K, Kumar B, Zhang Y, et al. A functional screen identifies miRNAs that inhibit DNA repair and sensitize prostate cancer cells to ionizing radiation. *Nucleic Acids Res*. 2015;43(8):4075-4086.
31. Bottai G, Pasculli B, Calin GA, Santarpia L. Targeting the microRNA-regulating DNA damage/repair pathways in cancer. *Expert Opin Biol Ther*. 2014;14(11):1667-1683.
32. Li Z, Rana TM. Therapeutic targeting of microRNAs: current status and future challenges. *Nat Rev Drug Discov*. 2014;13(8):622-638.
33. Rupaimoole R, Slack FJ. MicroRNA therapeutics: towards a new era for the management of cancer and other diseases. *Nat Rev Drug Discov*. 2017;16(3):203-222.